Supporting Information for

Structural characterization of the caveolin scaffolding domain in association with cholesterol-rich membranes

Cody L. Hoop, V. N. Sivanandam, Ravindra Kodali, Matthew N. Srnec, Patrick C.A. van der Wel

Department of Structural Biology, University of Pittsburgh School of Medicine, Biomedical Science Tower 3, 3501 Fifth Ave, Pittsburgh, Pennsylvania 15260, USA

Table S1 - Sequences, labeling schemes, and amounts of isotopically labeled peptides used for the MAS ssNMR samples (in 1:1 POPC/cholesterol). Labeled residues are underlined in the primary sequence.

ID	Labeling	Sequence	Peptide amount (mg)
p1	U-^{13}C,^{15}N-[A_{87}, F_{92}, V_{94}, K_{96}]	DGIWK<u>A</u>SFTT<u>F</u>T<u>V</u>T<u>K</u>YWFYRLLSALFGI (Cav_{82-109})	3.7
p2	U-^{13}C,^{15}N-[G_{83}, V_{94}, F_{99}, L_{102}, A_{105}]	D<u>G</u>IWKASFTTFT<u>V</u>TKYW<u>F</u>YR<u>L</u>LS<u>A</u>LFGI (Cav_{82-109})	2.65
p3	U-^{13}C,^{15}N-[G_{83}, A_{87}]	EGTHSFD<u>G</u>IWK<u>A</u>SFTTFTVTKYWFYRLLSALFGI (Cav_{76-109})	3.6

Table S2 - Detailed experimental conditions of 1D and 2D NMR experiments shown in the main text and supporting information. Abbreviations: NS, number of scans per t_1 point; Temp., temperature of cooling gas; MAS, magic angle spinning rate; RD, recycle delay; TPPM, ^{1}H decoupling power during evolution and acquisition (using two-pulse phase modulation scheme).

2D Spectra									
Figure	**Sample**[a)]	**Experiment**	**NS**	**Temp (K)**	**MAS (kHz)**	**RD (s)**	**TPPM during acq. (kHz)**	**t_1 evol. (ms)**	**Mixing (ms)**
4, S3	p1	DARR 2D	152	283	8	3.5	83	256x31.25	25
4	p2	DARR 2D	152	283	8	3.5	83	256x31.25	25
5	p1	PDSD 2D	104	283	8	3	71	256x31.25	400
5	p2	PDSD 2D	152	283	8	3	83	256x25.00	400
S3	p3	DARR 2D	144	283	8	3	83	283x32.00	25

[a)] All 2D spectra were acquired on 10 mol% of the respective peptide in 1:1 (molar ratio) POPC/cholesterol membranes.

1D Spectra							
Figure	**Sample**	**Experiment**	**NS**	**Temp (K)**	**MAS (kHz)**	**RD (s)**	**TPPM during acq. (kHz)**
2	1:1 POPC (6.3mg) /Chol (3.2mg)	^{1}H-^{13}C CP	2560	283	8	3.5	83
2	10mol% na-Cav_{82-109} (6mg) in 1:1 POPC (6.2mg)/Chol (3.1mg)	^{1}H-^{13}C CP	2560	283	8	3.5	83
2	10mol% na-Cav_{83-102} (6.75mg) in 1:1 POPC (9.14mg)/Chol (4.59mg)	^{1}H-^{13}C CP	5120	300	8	3.5	50
2	POPC (5mg)	^{31}P 1D	3072	300	0	3.5	50
2	10mol% p1 in POPC (4.47mg)	^{31}P 1D	3072	300	0	3.5	50
2	1:1 POPC (6.3mg)/Chol	^{31}P 1D	2048	300	0	3.5	50
2	10mol% na-Cav_{83-102} in 1:1 POPC (9.14mg)/Chol	^{31}P 1D	6144	300	0	3.5	50
2, S1	10mol% p1 in 1:1 POPC (7.08mg)/Chol	^{31}P 1D	2048	300	0	3.5	50
S1	10mol% p1 (6.8mg) in 1:1 POPC (7.08mg) /Chol (3.56mg)	^{1}H-^{13}C CP	1024	283	8	3	71.5
S1	2mol% p1 (2.15mg) in 1:1 POPC (12.16mg)/Chol (6.11mg)	^{1}H-^{13}C CP	4096	283	8	3.5	83
S1	10mol% p1 (2.15mg) in POPC (4.47mg)	^{1}H-^{13}C CP	4096	283	5	3.5	83
S1	2mol% p1 in 1:1 POPC (12.16mg) /Chol	^{31}P 1D	2048	300	0	3	50

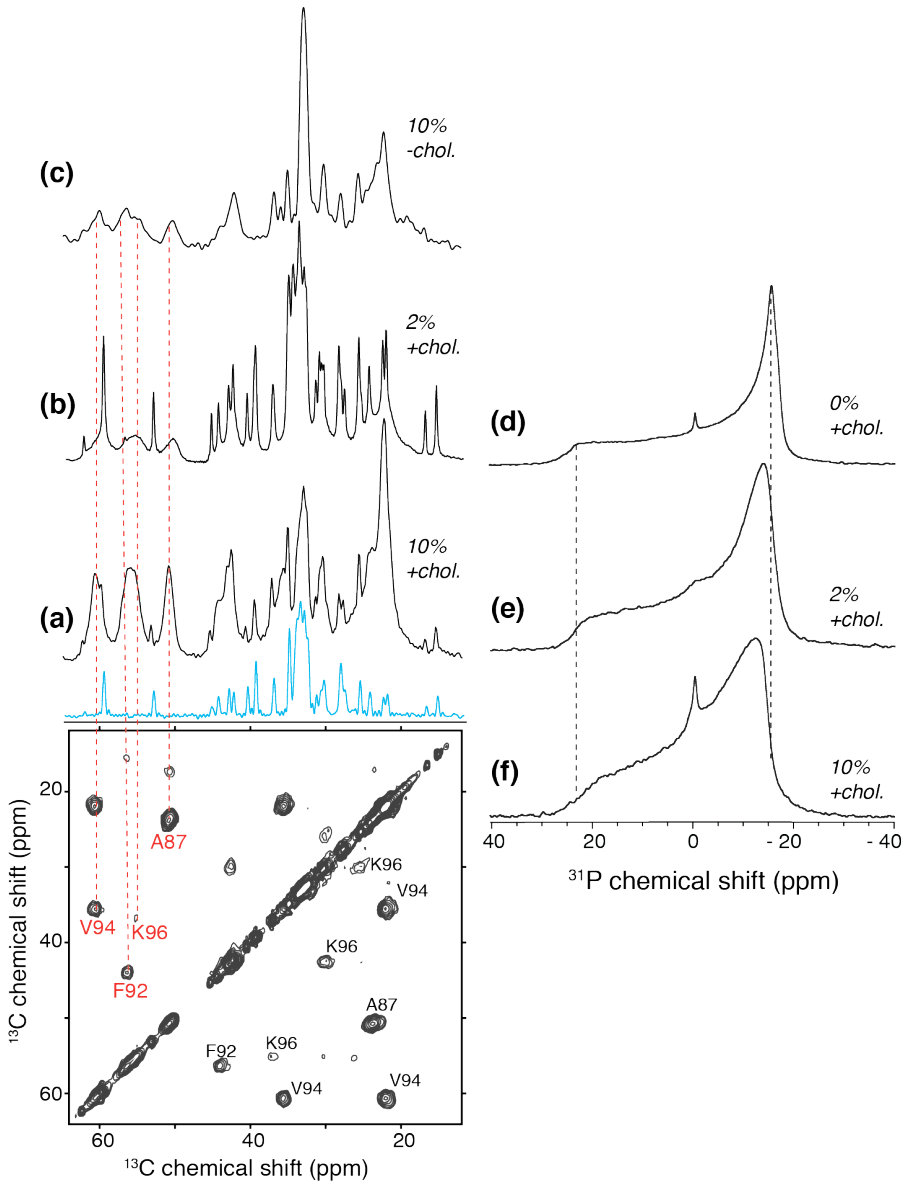

Figure S1 – (a-c) Comparison of ^{13}C 1D spectra: (a) 10mol% $Cav_{82\text{-}109}$ in 1:1 POPC/cholesterol, (b) 2mol% $Cav_{82\text{-}109}$ in 1:1 POPC/cholesterol, (c) 10mol% $Cav_{82\text{-}109}$ in pure POPC. A 1:1 POPC/cholesterol ^{13}C spectrum is provided in cyan for reference of lipid and cholesterol signals (ref. Figure 2 for specific assignments). The ^{13}C-^{13}C DARR 2D (from Fig. 4) shows the peptide assignments (10 mol% in POPC/cholesterol). The most visible Cα signals are marked in red. (d-f) Comparison of ^{31}P lineshapes with increasing concentrations of $Cav_{82\text{-}109}$. (d) 1:1 POPC/cholesterol in absence of peptide, (e) 2mol% $Cav_{82\text{-}109}$ in 1:1 POPC/cholesterol, and (f) 10mol% $Cav_{82\text{-}109}$ in 1:1 POPC/cholesterol. A concentration-dependent narrowing of the ^{31}P CSA is observed upon addition of peptide.

Table S3 - Secondary structure content estimates from FTIR. The relative amounts of α-helix and β-sheet content of both peptides (Cav_{82-109} and Cav_{83-102}) in POPC/cholesterol were estimated by deconvolution of the FTIR spectra as shown in Figure S2 and Figure 3.

Sample	α-helix (%)	β-sheet (%)
10mol% Cav_{82-109}	63	37
10mol% Cav_{83-102}	11	89
5mol% Cav_{82-109}	56	44
5mol% Cav_{83-102}	15	85

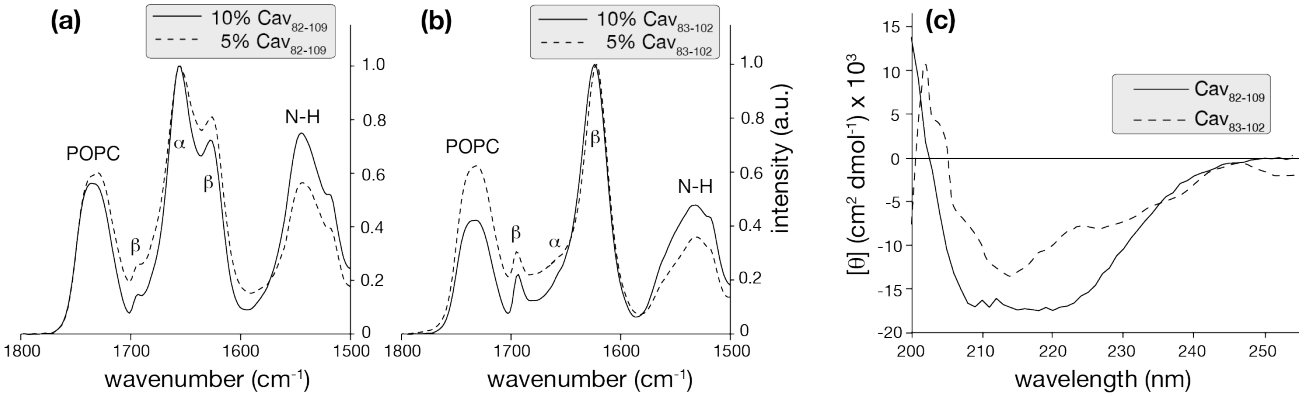

Figure S2 – Additional FTIR and CD data. FTIR spectra for (a) Cav_{82-109} and (b) Cav_{83-102} in 1:1 POPC/cholesterol. For each peptide, the resulting data with 10mol% peptide (solid) and 5mol% peptide (dashed) is shown. Relative amounts of α-helix and β-strand structure have been estimated by peak deconvolution and are tabulated in table S3, above. (c) CD spectra of 25uM Cav_{82-109} (solid) and 10uM Cav_{83-102} (dashed) in POPC at a 1:100 peptide-to-lipid ratio at 25ºC. Although poor spectral quality due to scattering prevented a reliable quantitative analysis, it is clear there is an increase in helical structure in the longer peptide as previously reported in DPC by Le Lan et al. (1).

Table S4 - ^{13}C chemical shift resonances for Cav1 peptides obtained by solid state MAS NMR. Entries for residues A87 and V94 include the shifts of a minor secondary population (ref. main text). Chemical shifts are referenced relative to aqueous DSS through indirect referencing to external adamantane. The last column summarizes the secondary structure assignments (see main text).

	Res.	**Cα**	**Cβ**	**Cγ**	**Cδ(1)**	**Cδ2**	**Cε**	**CO**	
Caveolin Scaffolding Domain	G83	46.47±0.04						170.5±0.07	-
	A87	50.6±0.21	23.6±0.16					176.0±0.18	β
		50.61±0.01	22.60±0.06					176±0.18	β
	F92	56.3±0.15	43.9±0.21	139.2±0.12	132.4±0.01		131.5±0.03	174.3±0.24	β
	V94	60.5±0.21	35.5±0.16	22.0±0.14				173.9±0.28	β
			32.0±0.40	21.8±0.12					
	K96	55.0±0.24	37.1±0.33	25.9±0.46	29.9±0.18		42.5±0.14	174.1±0.25	β
	F99		38.8±0.1	131.2±0.09					α
IMD	L102	58.3±0.12	41.6±0.16	27.3±0.09	25.1±0.09	23.6±0.22		178.1±0.22	α
	A105	54.5±0.22	18.9±0.09					179.2±0.35	α

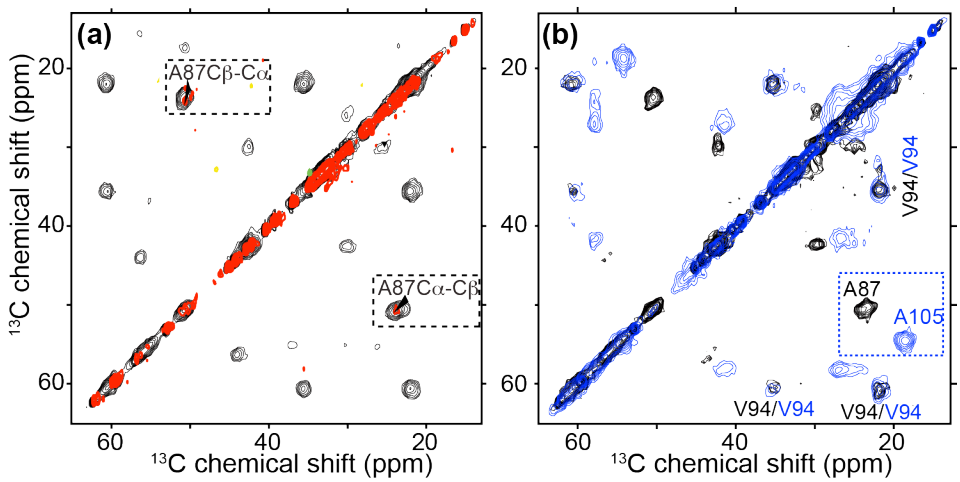

Figure S3 - Overlay of 2D ^{13}C-^{13}C ssNMR spectra of different samples. Shown is the intra-aliphatic region of spectra with 25 ms DARR mixing, providing 1-2 bond transfers. Panel (a) compares the 28- and 34-residue long peptides p1 (black) and p3 (red), where A87 in the CSD is uniformly ^{13}C-labeled in both. The Cα and Cβ chemical shifts are unchanged and are indicative of β-sheet secondary structure. In (b), we compare peptides p1 (black) and p2 (blue), showing that the V94 shifts are reproducible, but the two Ala residues in the CSD (A87) and intramembrane domain (A105) have very different shifts due to the difference in secondary structure. Spectra were obtained at 600 MHz ^{1}H frequency, 8 kHz MAS and at 283 K.

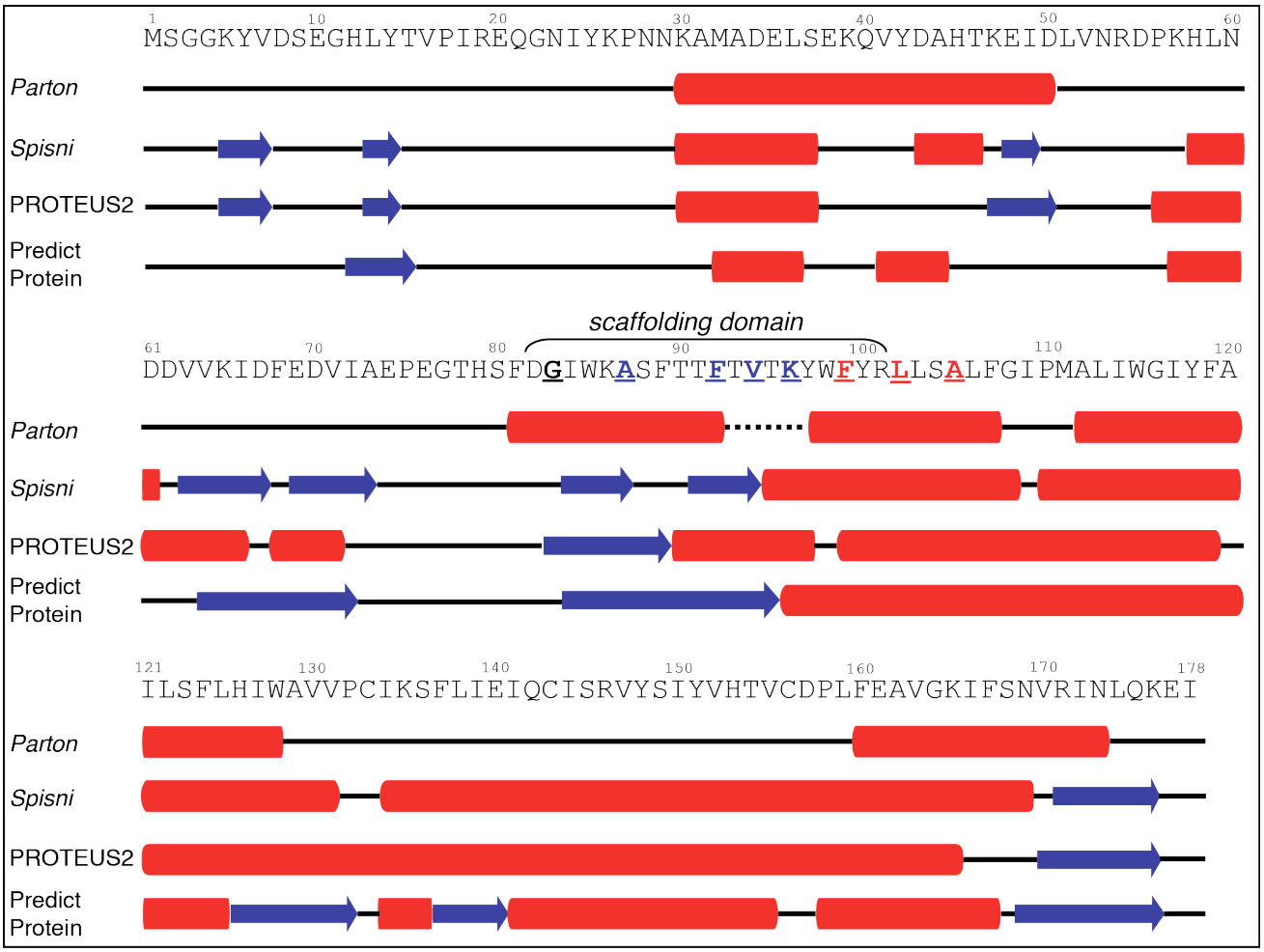

Figure S4 – Schematic illustrations of secondary structure predictions for full-length Cav1. Parton et al. (top row) have presented an all-helical model based on primary sequence analysis (2). In a bioinformatics study, Spisni et al. used an array of algorithms to obtain a model in which residues 84-94 form an anti-parallel β-hairpin(3). In our hands, the PSIPRED (in main text; Fig. 6), PROTEUS2, and PredictProtein algorithms predict significant β-sheet secondary structure, although with slightly varying distributions. Predictions of β-structure within the CSD by the PSIPRED, PredictProtein and Spisni models quite closely match our experimental observations on the CSD-containing Cav1 fragments, as marked by color-coding on the primary sequence (also see Fig. 5 and 6).

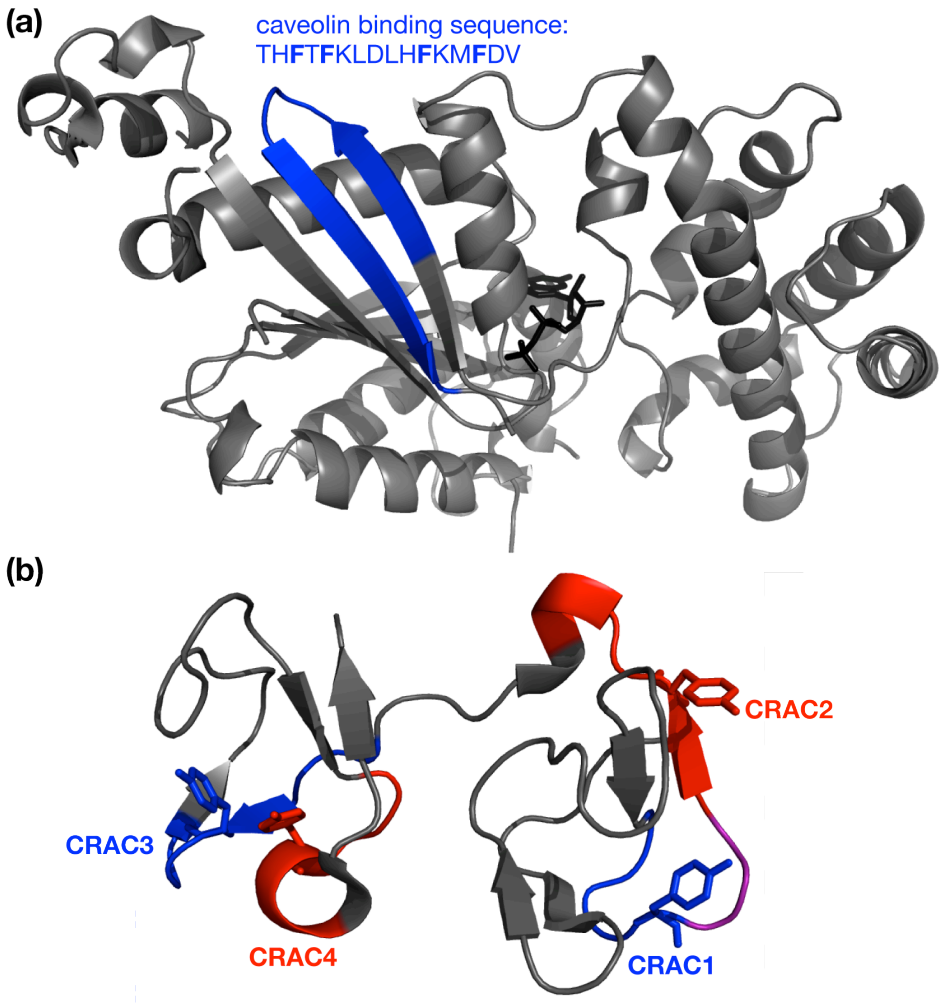

Figure S5 – (a) Structure of rat Giα1 with GDP bound (black sticks) (4), a binding partner of caveolin (5). The caveolin binding sequence is shown in blue, and has apparent homology to a motif within caveolin itself (6). (b) Structure of PDC-109, showing its four putative CRAC motifs. The CRAC motifs are alternatingly colored blue and red (overlapping residues in purple). The Tyr residues at the heart of each CRAC motif are shown in stick representation. Note the variation in (secondary) structure between the different motifs, but also that the structure is not necessarily α-helical. Two motifs contain anti-parallel β-sheet structures, one of which (CRAC2) is flanked by a short helix as commonly found for CRAC motifs (although in this case not transmembrane). These figures were prepared using PyMol (Schrödinger).

References cited in the Supporting Information

1. Le Lan, C., Neumann, J. M., and Jamin, N. (2006) *FEBS Lett* **580**, 5301-5305
2. Parton, R. G., Hanzal-Bayer, M., and Hancock, J. F. (2006) *J Cell Sci* **119**, 787-796
3. Spisni, E., Tomasi, V., Cestaro, A., and Tosatto, S. C. E. (2005) *Biochem Biophys Res Commun* **338**, 1383-1390
4. Coleman, D. E., and Sprang, S. R. (1998) *Biochemistry* **37**, 14376-14385
5. Li, S., Okamoto, T., Chun, M., Sargiacomo, M., Casanova, J. E., Hansen, S. H., Nishimoto, I., and Lisanti, M. P. (1995) *J Biol Chem* **270**, 15693-15701
6. Couet, J., Li, S., Okamoto, T., Ikezu, T., and Lisanti, M. P. (1997) *J Biol Chem* **272**, 6525-6533